





Dynamics of epidemics from cavity master equations: Susceptible-infectious-susceptible modelsErnesto Ortega , David Machado , and Alejandro Lage-Castellanos ^{*}
Complex Systems Group, Physics Faculty, Havana University, 10400 Havana, Cuba (Received 18 March 2021; accepted 27 January 2022; published 17 February 2022)

We apply the recently introduced cavity master equation (CME) to epidemic models and compare it to previously known approaches. We show that CME seems to be the formal way to derive (and correct) dynamic message passing (rDMP) equations that were previously introduced in an intuitive *ad hoc* manner. CME outperforms rDMP in all cases studied. Both approximations are nonbacktracking and this causes CME and rDMP to fail when the ecochamber mechanism is relevant, as in loopless topologies or scale free networks. However, we studied several random regular graphs and Erdős-Rényi graphs, where CME outperforms individual based mean field and a type of pair based mean field, although it is less precise than pair quenched mean field. We derive analytical results for endemic thresholds and compare them across different approximations.

DOI: [10.1103/PhysRevE.105.024308](https://doi.org/10.1103/PhysRevE.105.024308)**I. INTRODUCTION**

Since the seminal works introducing susceptible-infectious-recovered compartment models (SIR) of Kermack and McKendric [1], epidemics modeling has grown fast as a field. The approach has changed with time, from dynamical systems or population dynamics towards more stratified approaches as patchy, mobility based, age-structured, or contact matrices compartment models.

The current context of a global COVID-19 pandemic and the perspective of a coexistence with an endemic virus requires a test-trace-isolate epidemiological system to keep the outbreak controlled. Much attention is now put on agent based models [2–4] that could improve the efficacy of the testing strategy. Assuming that new technologies can provide reliable contact data between humans, the likelihood of people being infected needs to be estimated either by numerical simulations or some statistical modeling. To this end, it is suitable to count with fast algorithms that can accurately predict probabilities of infection for agents in networks.

There are a wide variety of such algorithms. The classical approach to the forecasting of epidemics on networks is an averaging of the master equation of the process complemented by a factorization assumption at some level. This yields a hierarchy of ever more complex but more accurate differential equations for expected values and correlations [5,6]. Most of the time only the first two levels, known as individual based mean field and pair based mean field, are used.

More recently, ideas from discrete optimization algorithms have sneaked into the inference of SIR kind of models in the shape of dynamical message passing [7,8] or belief propagation (BP) [9,10]. The main difference with respect to the previous approach is the appearance of conditional—rather than multivariate—probabilities to be integrated in time. It has been used with success in the reconstruction of epidemics

on graphs and it is currently being tried in the task of risk assessment for COVID-19 [11,12]. However, these two types of approaches—the standard master equations and the message passing one—have remained similar but theoretically disconnected.

It is known that a BP fixed point is connected to the cavity method from statistical mechanics [13]. An extension of the cavity method to continuous time Markov chain processes within discrete spin systems has been recently achieved through the derivation of a set of differential equations for cavity conditional probabilities: the cavity master equation (CME) [14]. In this article we explore CME's application to susceptible-infectious-susceptible (SIS) models in graphs (Sec. III) and compare it with Monte Carlo simulations and with well established mean-field approaches and dynamic message passing (rDMP). We will show that CME somehow binds both approaches, since it starts from a master equation, but produces message passing-like equations. CME seems to be the formal path to obtaining (and fixing) the dynamic message passing for recurrent models of epidemics rDMP [8] that were formerly presented in an *ad hoc* manner. Therefore, we retain the main contribution of this work to be methodological.

In some simple cases we draw analytical results for a group of steady state quantities and the corresponding critical spreading rate (Sec. IV). We also explore the average case dynamics of these equations, in particular in random regular and Erdős-Rényi graphs (Sec. V). Limitations of CME are discussed throughout the paper and the pros and cons are outlined in the Conclusions (Sec. VI).

II. EPIDEMICS ON NETWORKS

In what follows we focus on continuous time compartment epidemic models on networks. We assume a fixed network of contacts to be given $G = (V, E)$ with a set of vertices $V = \{1, 2, \dots, N\}$ and a set of edges E . An edge (i, j) is present if nodes i and j are neighbors in the network, meaning there is a possibility of transmission of diseases between both nodes.

^{*}ale.lage@gmail.com

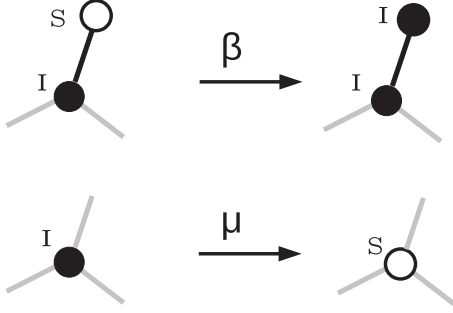


FIG. 1. Allowed transitions in SIS compartment model on networks.

The standard susceptible-infectious-susceptible model (SIS) considers the nodes to be in either of two compartments (states), $X_i = 0 \equiv$ susceptible or $X_i = 1 \equiv$ infectious, and is the simplest standard for recurrent transmissible diseases. The epidemic is thus a continuous time stochastic process with only two admitted transitions occurring at (i) rate β , at which a link (i, j) can transmit the state 1 from node i to j , and (ii) rate μ at which state 1 decays to state 0 on any infectious node, as represented in Fig. 1. An analytical description of this stochastic process is given by the master equation for the evolution in time of the probability over the whole configuration space $P(X_1, \dots, X_N, t)$ [6]. However, concise and exact, the integration in time of such an equation is generally impractical given the size 2^N of the configuration space.

Attempts to reduce the complexity start from factorizing the single master equation into many equations for each node marginals $P_i(X_i, t)$. Given that the X 's are two-state variables, $P_i(X_i)$ is parametrized by the mean value $E[X_i] = P_i(X_i = 1)$. This results in an equation that is still exact [6],

$$\frac{dE[X_i(t)]}{dt} = E \left[-\mu X_i(t) + \beta S_i(t) \sum_{j=1}^N a_{ij} X_j(t) \right], \quad (1)$$

where a_{ij} are the elements of the adjacency matrix, meaning that $a_{ij} = 1$ if nodes i and j are neighbors $[(i, j) \in E]$ and is zero otherwise.

However, the expectation value on the right hand side acts over products of variables $X_i(t)S_j(t)$, which requires a differential equation for the evolution of the correlations. Not surprisingly, the two point correlation functions depend on three point correlations and so on and so forth.

The simplest closure of Eq. (1) is the individual-based mean field (IBMF) in which independence is assumed as $E[X_i(t)S_j(t)] \approx E[X_i(t)]E[S_j(t)] \equiv \rho_i(t)\varrho_j(t)$ (ϱ_i is the probability that node i is susceptible) and therefore Eq. (1) is now a closed set of nonlinear differential equations:

$$\frac{d\rho_i(t)}{dt} = -\mu\rho_i(t) + \beta[1 - \rho_i(t)] \sum_{j \in \partial i} \rho_j(t), \quad (2)$$

where we used the notation ∂i to represent the set of neighbors of node i .

The second simplest closure is the one known as the pair based mean field (PBMF), in which two point correlations are

treated analytically [15–18],

$$\begin{aligned} \frac{dE[X_i S_j]}{dt} &= -2\mu E[X_i S_j] + \mu E[X_i] + \beta \sum_{k=1}^N a_{ik} E[S_i S_j X_k] \\ &\quad - \beta \sum_{k=1}^N (a_{jk}) E[X_i S_j X_k], \end{aligned} \quad (3)$$

but a factorization is assumed for higher correlations. Different approaches have been used to approximate $E[X_i S_j X_k]$ in terms of smaller correlations. In this paper we will compare with the approximations proposed in [15] $E[X_i S_j X_k] \approx E[X_i S_j]E[X_k] \equiv \phi_{ij}(t)\rho_k(t)$,

$$\frac{d\rho_i(t)}{dt} = -\mu\rho_i(t) + \beta \sum_{j \in \partial i} \phi_{ij}(t), \quad (4)$$

$$\begin{aligned} \frac{d\phi_{ij}(t)}{dt} &= -(2\mu + \beta)\phi_{ij}(t) + \mu\rho_i(t) - \beta\phi_{ij}(t) \sum_{k \in \partial j \setminus i} \rho_k(t) \\ &\quad + \beta[1 - \rho_i(t) - \phi_{ij}(t)] \sum_{k \in \partial i \setminus j} \rho_k(t), \end{aligned} \quad (5)$$

and [16] (pair quenched mean field) $E[X_i S_j X_k] \approx \frac{E[X_i S_j]E[S_j X_k]}{E[S_j]} \equiv \frac{\phi_{ij}(t)\phi_{kj}(t)}{\rho_j(t)}$,

$$\begin{aligned} \frac{d\rho_i(t)}{dt} &= -\mu\rho_i(t) + \beta \sum_{j \in \partial i} \phi_{ji}(t), \\ \frac{d\phi_{ij}(t)}{dt} &= -(2\mu + \beta)\phi_{ij}(t) + \mu\rho_i(t) - \beta\phi_{ij}(t)/[1 - \rho_j(t)] \\ &\quad \times \sum_{k \in \partial j \setminus i} \phi_{kj}(t) + \beta[1 - \rho_j(t) - \phi_{ij}(t)]/[1 - \rho_i(t)] \\ &\quad \times \sum_{k \in \partial i \setminus j} \phi_{ki}(t). \end{aligned} \quad (6)$$

We will refer to the two different approximations shown in (5) and (6) as PBMF-1 and PBMF-2, respectively.

In both approaches, IBMF and PBMF, the expected values evolving in time are intended to be expectations over different stochastic stories of the whole epidemic process. Therefore, they are to be compared with averages over many Monte Carlo simulations of such a process.

A slightly different approach to modeling epidemics on graphs comes from message-passing inspired methods. The dynamic message passing [7,8] involves a set of probabilities and a set of conditional probabilities, rather than correlations [8]:

$$\frac{dp_i}{dt} = -\mu p_i + \beta(1 - p_i) \sum_k p_{ki}, \quad (7)$$

$$\frac{dp_{ij}}{dt} = -\mu p_{ij} + (1 - p_j)\beta \sum_{k \in \partial i \setminus j} p_{ki}, \quad (8)$$

where $p_i = E[X_i]$ similarly as before, but $p_{ij} \equiv P(X_i = 1 | X_j = 0)$ is a conditional probability resembling the kind of cavity fields or messages that commonly appear in the cavity method and the belief propagation algorithm for discrete optimization.

The main results of this article are drawn from the cavity master equation [14]. They are quite similar to those of rDMP and help in formalizing this rather empirical approach by deriving it from a more solid mathematical setting. In doing so we do not only correct one term of the rDMP equations, but also underline the approximations involved and therefore shed light on possible improvements.

III. CAVITY MASTER EQUATIONS FOR SIS EPIDEMICS

In order to connect with its first presentation in [14], we start by considering the general continuous time dynamics of a system $\sigma = \{\sigma_1, \dots, \sigma_N\}$ of N bimodal variables $\sigma_i \in \{\pm 1\}$ interacting with their neighbors in some given topology. In the very generic Markovian case, the dynamic is fully defined by the rate function $r_i(\sigma)$ at which variables flip their states from $\sigma_i \rightarrow -\sigma_i$. The distribution $P(\sigma, t)$ in the configuration space of this stochastic process is ruled by the joint master equation:

$$\frac{dP(\sigma)}{dt} = - \sum_{i=1}^N [r_i(\sigma)P(\sigma) - r_i(F_i(\sigma))P(F_i(\sigma))], \quad (9)$$

$$\frac{dP(\sigma_i)}{dt} = - \sum_{\sigma_{\partial i}} \left[r_i(\sigma_i, \sigma_{\partial i}) \left(\prod_{k \in \partial i} p(\sigma_k | \sigma_i) \right) P(\sigma_i) - r_i(-\sigma_i, \sigma_{\partial i}) \left(\prod_{k \in \partial i} p(\sigma_k | -\sigma_i) \right) P(-\sigma_i) \right], \quad (10)$$

$$\frac{dp(\sigma_i | \sigma_j)}{dt} = - \sum_{\sigma_{\partial i \setminus j}} \left[r_i[\sigma_i, \sigma_{\partial i}] \left(\prod_{k \in \partial i \setminus j} p(\sigma_k | \sigma_i) \right) p(\sigma_i | \sigma_j) - r_i[-\sigma_i, \sigma_{\partial i}] \left(\prod_{k \in \partial i \setminus j} p(\sigma_k | -\sigma_i) \right) p(-\sigma_i | \sigma_j) \right]. \quad (11)$$

We have lightened the notation by not putting the i and ij dependence of the distributions, understanding that they assume the index of the variables they depend on [as $P(\sigma_i) \equiv P_i(\sigma_i, t)$ and $p(\sigma_i | \sigma_j) \equiv p_{i,j}(t, \sigma_i | \sigma_j)$]. Both probabilities are intended in the sense “over the ensemble of dynamic evolutions up to time t ,” starting from the same initial conditions.

This is a substantial improvement over the original master equation since we are dealing now with N functions $P_i(\sigma_i, t)$ representing the distribution of variables σ_i , and with $N * \langle k \rangle$ functions $p_{(i,j)}(\sigma_i | \sigma_j, t)$ that represent the probability of finding variables in a given state, conditioned to the state of one of its neighbors ($\langle k \rangle$ is the average degree of the nodes in the interactions network). In the worst case of a fully connected system, we still would have $O(N^2)$ equations, that can be numerically integrated even for relatively large systems, compared to what we can do with Eq. (9).

We can readily translate the cavity master equations (10) and (11) to the case of the SIS epidemic model by identifying our two states as $S \rightarrow \sigma_i = -1$ and $I \rightarrow \sigma_i = 1$. After complementarity [$P_i(I) + P_i(S) = 1$], it is enough to track the infection probability in each node $P_i(I)$. The first term in Eq. (10) largely simplifies due to the fact that the recovery rate $r_i(\sigma_i = 1, \sigma_{\partial i}) = \mu$ is independent of the neighbors' state, resulting in $-\mu P(I)$. Considering also that the transmission rates are additive $r_i(S, \sigma_{\partial i}) = \sum_{k'} r_i(S, \sigma_{k'})$ and that $r_i(S, S) = 0$ and $r_i(S, I) = \beta$, we get to the cavity master equations for the SIS model

where F_i represents the flip operator on variable i , i.e., $F_i(\sigma) = \{\sigma_1, \dots, \sigma_{i-1}, -\sigma_i, \sigma_{i+1}, \dots, \sigma_N\}$.

Although exact, the previous equation is useless already for middle size systems, since it actually represents a set of 2^N coupled differential equations that take exponential time to enumerate, let alone to integrate. However, this is the correct starting point for approximations, as is usually done to obtain mean-field equations (2), (4), (5), and (6) in epidemics models [5,6,19].

In [14] this master equation is recast into an equilibrium problem by extending the configuration space to consider the continuous trajectory of each variable in time $\mathbf{X} = \{X_1, \dots, X_N\}$, where $X_i = \{\sigma_i(t) : \forall t \in [0, T]\}$. Although at a glance it seems untreatable the infinite dimensional space for the functions $X_i(t)$, the discrete values of $\sigma_i(t)$ allow for a codification of the functions in a number of transition times $\{T_1^{(i)}, T_2^{(i)}, \dots\}$ such that $\sigma_i(T_k^{(i)}) = -\sigma_i(T_{k-1}^{(i)} + dt)$. The resulting random point process is treated with standard techniques in equilibrium statistical mechanics to write down a closed set of cavity master equations as

as

$$\frac{dp_i}{dt} = -\mu p_i + \beta(1 - p_i) \sum_k p_{ki}, \quad (12)$$

$$\frac{dp_{ij}}{dt} = -\mu p_{ij} + (1 - p_{ij}) \beta \sum_{k \in \partial i \setminus j} p_{ki}, \quad (13)$$

where we simplified the notation further by making $P(\sigma_i = 1) \equiv p_i$ and $P(\sigma_i = 1 | \sigma_j = -1) \equiv p_{ij}$. Appendix A contains a more detailed derivation of these equations for the SIS model. Equations (12) and (13) are almost identical to rDMP (7) and (8), except for the very last term where $(1 - p_j)$ is replaced by $(1 - p_{ij})$. In particular, the linearized version of Eq. (13) is equal to that of (8), resulting in the same endemic thresholds for either method.

The integration of both approximations might not be too different in certain cases. For instance, for an SIS epidemic outbreak in Zacharia's karate club network (following [8]), starting at node 1 both approaches are quite similar as shown in Fig. 2 (left). In Fig. 2 (right) the $L1$ distance between the average from many Monte Carlo simulations and the predictions made by all four methods CME, rDMP, IBMF, and PBMF show features that will repeat in other benchmarks: (i) that both rDMP and CME get the general qualitative behavior well, (ii) with a rather faster outbreak expansion in the transient, compared to Monte Carlo simulations, and (iii) with CME better fitting the stationary state, and quite close (exactly the same for regular graphs) to PBMF-2.

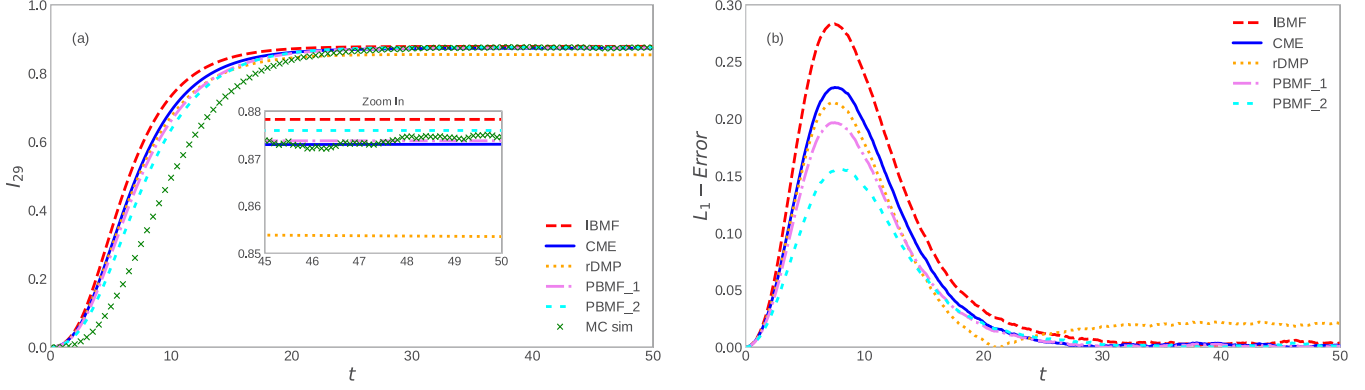


FIG. 2. (a) Probability of node 29 to be infected as a function of time, discounting at each time the situations in which the epidemics disappear. The epidemic outbreak was in node 1, with $\beta = 0.1$ and $\mu = 0.05$. The inset is a closer look in the stationary state. (b) L_1 distance between the four approximations IBMF, PBMF, rDMP, and CME with respect to 10^5 Monte Carlo (MC) simulations.

Individual based mean field tends to be the fastest growing prediction. Overall, PBMF-2 seems to be the most accurate approximation, both for the transient and the steady.

When computing the Monte Carlo averages we have neglected the simulations in which the epidemic is randomly wiped out in the first few iterations. None of these methods can take these fluctuations into account, since they are all mean-field approaches.

Differences are more evident in the case of random regular graphs with degree $k = 3$ in Fig. 3. We represent the average epidemic size, i.e., the fraction of infected nodes with respect to $N = 1000$, the number of nodes in the graph at every time step. We started from a fraction $\alpha = 0.5$ of nodes infected and observed the onset of the endemic state.

Limitations: Nonbacktracking

It has already been underlined that message passing–like equations are not particularly suited for SIS models [20], since they are naturally nonbacktracking, and therefore miss the existing ecochamber transmission, a handicap absent in mean-field approximations. It is important to emphasize that the present approach, although correcting rDMP and improving it, still has this handicap.

Consider, for instance, the integration of our equations in a star model, where a central node, name it 0, is connected to N nodes around it. While both Monte Carlo simulations and mean-field approximations predict a long lasting epidemic (depending on β , μ , and N), CME and rDMP equations will rapidly converge to zero, regardless of β , μ , and N . This is easy to check, since, for instance, the equation for the central node 0 will read

$$\frac{dp_0}{dt} = -\mu p_0$$

as all messages from the leaves of the star p_{k0} are identically zero. This situation, that may seem exceptional, is fundamental in scale free graphs, where hub nodes keep getting reinfected by their immediate partners, that eventually leads to infect them back (ecochamber).

For a similar reason, neither rDMP nor CME will predict a sustained epidemic in a tree, while Monte Carlo simulations and mean-field methods do. We have checked these facts, discussed in [20], numerically. It is surprising that the approximation, nevertheless, gives some accurate predictions in graphs with loops where the ecochamber transmission is not the relevant mechanism.

IV. ENDEMIC (STEADY) STATE

We analytically compute the epidemic size in the endemic state for these approximations for random regular graphs. Since every node has the same degree k , the equations are similar for every node, and we can assume that in the steady state the topology is averaged out, and all the probabilities are the same, regardless of the node indexes.

Working explicitly for the CME approximation, stationarity means we have to set $\frac{dp_i}{dt}$ and $\frac{dp_{ij}}{dt}$ to 0 in Eqs. (12) and (13):

$$\begin{aligned} \mu p_i &= \beta(1 - p_i) \sum_k p_{ki} \equiv \beta(1 - p_i) k p_{ij}, \\ \mu p_{ij} &= (1 - p_{ij}) \beta \sum_{k \in \partial i \setminus j} p_{ki} \equiv (1 - p_{ij}) \beta (k - 1), \end{aligned} \quad (14)$$

where now the indices i and i, j are generic. Solving this system of equations we get, for the two variables p_i and p_{ij} ,

$$p_i = \frac{\lambda(k - 1) - 1}{\lambda(k - 1) - 1 + (k - 1)/k}, \quad p_{ij} = 1 - \frac{\mu}{(k - 1)\beta}. \quad (15)$$

This can be already tested against simulations of random regular graphs. Furthermore, we can obtain the spreading rate or effective infection rate $\lambda = \beta/\mu$ above which there is an endemic outbreak (sustained in time epidemic) by solving $p_i(k) = 0$, resulting in the epidemic threshold $\lambda_c = 1/(k - 1)$. A similar procedure for all five approximations results in Table I. Notably, in spite of being different in the transient, the pair-based mean-field 2 approach coincides in the stationary state with the cavity master equation.

The critical values $\lambda_c = 1/k$ for IBMF are consistent with those in [21] and citations therein with similar approaches.

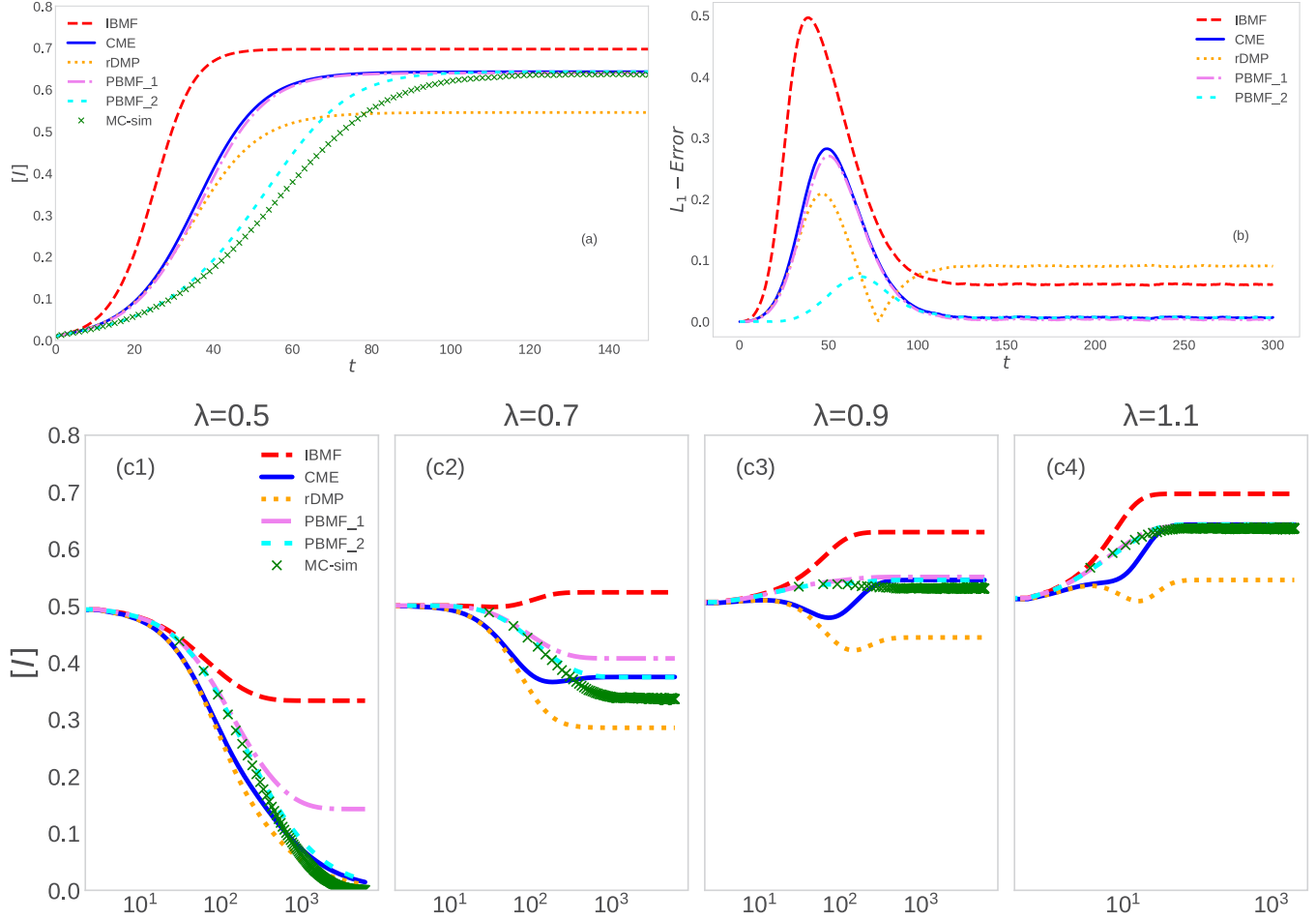


FIG. 3. Random regular graph with connectivity $k = 3$. *Top figures*: percent of the population in the infected state (a) and the L_1 distance (b), in a graph of 1000 nodes with parameters $\beta = 0.11$ and $\mu = 0.1$ and an outbreak in one node of the system. *Bottom figures*: (c1)–(c4) percent of the population in the infected state for different values $\lambda = \beta/\mu$ in a graph of 1000 nodes, starting with half of the population in the infected state. In all figures each point of MC is an average over 10^4 simulations.

PBMF-2, CME, and rDMP prediction $\lambda_c = 1/(k - 1)$, however, is known to be a second order correction to the endemic threshold [15,16], and it is numerically [16,22] seen to outdo the individual based value.

In Fig. 4 we present the analytical predictions of each approximation for the epidemic size p_i at the steady state

TABLE I. Steady state and epidemic threshold λ_c under four approximations (IBMF, PBMF, rDMP, and CME) on random regular graphs of connectivity k .

Approximation	Endemic state (equilibrium)	λ_c
IBMF	$p_i = 1 - \frac{1}{k\lambda}$	$\lambda_c = \frac{1}{k}$
PBMF-1	$p_i = \frac{k+k(k-1)\lambda-2/\lambda-1}{(k-1)(\lambda k+2)}$	$\lambda_c = \frac{\sqrt{1+\frac{8k}{k-1}}-1}{2k}$
PBMF-2	$p_i = \frac{\lambda(k-1)-1}{\lambda(k-1)-1+(k-1)/k}$	$\lambda_c = \frac{1}{k-1}$
rDMP	$p_i = 1 - \frac{1}{(k-1)\lambda}$ $p_{ij} = \frac{(k-1)\lambda-1}{k\lambda}$	$\lambda_c = \frac{1}{k-1}$
CME	$p_i = \frac{\lambda(k-1)-1}{\lambda(k-1)-1+(k-1)/k}$ $p_{ij} = 1 - \frac{1}{(k-1)\lambda}$	$\lambda_c = \frac{1}{k-1}$

as a function of λ . When compared to Monte Carlo results, mean-field approximations (IBMF and PBMF-1) give an overestimation of the epidemic size at small λ , and rDMP an underestimation at large λ . Meanwhile, CME and PBMF-2 seems to be a better prediction mixing the large λ behavior of IBMF and PBMF-1 with the small λ behavior of rDMP.

The results presented in Fig. 4 are very similar to those shown in [23] where a tractable master equation is presented for the evolution in time of the epidemic size in a graph with the same degree. This description has more resemblance with a degree based approximation and, as in our case, it catches with similar accuracy the value of the epidemic threshold for a random regular graph of connectivity 3.

V. AVERAGE CASE FOR UNCORRELATED HETEROGENEOUS GRAPHS

The systems of equations defining IBMF, PBMF, rDMP, and CME could be large and delicate to solve on a given graph, although a simple numerical integration normally works. However, in many cases we are interested in general predictions for certain families of graphs or topologies. In this section we derive an average version of the CME

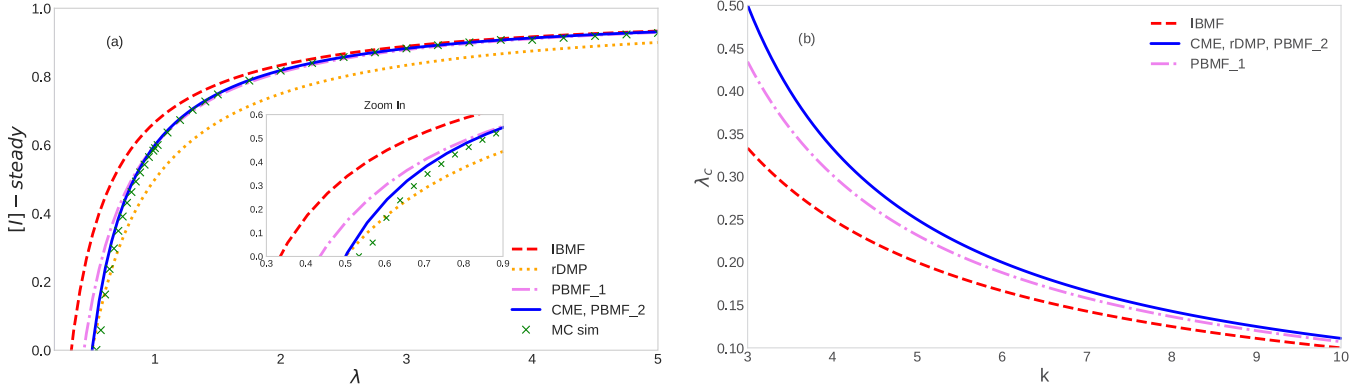


FIG. 4. (a) Comparison between Monte Carlo simulations and the predicted endemic equilibrium for each approximation as a function of λ for random regular graphs. Each MC point is an average of the last value of the probability of infected computed for 10^4 simulations over the 1000 nodes in the system. (b) Comparison between the epidemic threshold predicted by the methods as a function of graph connectivity.

approximation to characterize SIS epidemics on uncorrelated random graphs. Our approach relates closely to that in [24,25], based on IBMF approximation, where the prevalence at the stationary state is derived just above the epidemic threshold.

The simplest description of a graph ensemble is given by the distribution of degrees of its nodes. In the case of uncorrelated graphs, that distribution is the full description of the ensemble. One of the first theoretical approaches used for epidemic modeling on networks was the degree based mean-field approach (DBMF) [26]. It provided a set of master equations for the probability of a node of degree k to be infected at time t , assuming statistical equivalence of all nodes of degree k . As stated in [21] DBMF can be obtained by performing a degreewise average over the IBMF equations.

A similar procedure can be performed in the context of CME. Since the CME equations depend on the information coming from the neighbors in the network, it is expected that nodes more connected will have a different behavior than those less connected. We therefore attempt to reduce the number of equations in our system by characterizing all nodes with the same degree by a couple of average parameters

$$p^\gamma = \frac{1}{N^\gamma} \sum_{i:d_i=\gamma+1} p_i, \quad p_{\rightarrow}^\gamma = \frac{1}{M^\gamma} \sum_{i:d_i=\gamma+1} \sum_{j \in \partial i} p_{ij}^\gamma. \quad (16)$$

In both cases the normalization factors count the number of terms in the sums: N^γ is the number of nodes with degree $k = \gamma + 1$, while M^γ is the number of graph edges that contain one of these N^γ nodes.

Averaging Eqs. (12) and (13), and after some simplifications, we get the average CME:

$$\dot{p}^\gamma = -\mu p^\gamma + \beta(\gamma+1)(1-p^\gamma) \sum_{\gamma'} g(\gamma') p_{\rightarrow}^{\gamma'}, \quad (17)$$

$$\dot{p}_{\rightarrow}^\gamma = -\mu p_{\rightarrow}^\gamma + \beta\gamma(1-p_{\rightarrow}^\gamma) \sum_{\gamma'} g(\gamma') p_{\rightarrow}^{\gamma'}, \quad (18)$$

where $g(\gamma)$ is a contact degree distribution. A node extracted randomly from the set of nodes V has degree k with distribution $k \sim P(k)$. However, in order to average the CME equations we rather need to know the excess-degree distribution $g(\gamma)$ of nodes that are sampled by randomly picking up an edge $(i, j) \in E$. In the case of uncorrelated graphs, a known

result [21] relates degree and contact degree distribution by

$$g(\gamma) = \frac{(\gamma+1)P(\gamma+1)}{\sum_{\gamma} (\gamma+1)P(\gamma+1)}, \quad \gamma \in [0, 1, \dots]. \quad (19)$$

Following [26,27] we can obtain the endemic threshold in terms of $\Theta = \sum_{\gamma} g(\gamma) p_{\rightarrow}^\gamma$. In the stationary state $\dot{p}^\gamma = 0$ and $\dot{p}_{\rightarrow}^\gamma = 0$ in (17) and (18) lead to equations for p^γ and p_{\rightarrow}^γ as a function of Θ :

$$p^\gamma = \frac{\lambda(\gamma+1)\Theta}{1 + \lambda(\gamma+1)\Theta}, \quad p_{\rightarrow}^\gamma = \frac{\lambda\gamma\Theta}{1 + \lambda\gamma\Theta}. \quad (20)$$

Plugging the last equation into the definition of Θ , we obtain a self-consistent equation similar to the one in [26–28],

$$\Theta = f(\Theta) \equiv \sum_{\gamma} \frac{(\gamma+1)P(\gamma+1)}{\langle k \rangle} \frac{\lambda\gamma\Theta}{1 + \lambda\gamma\Theta}, \quad (21)$$

which always has a disease-free solution $\Theta = 0$. This solution becomes unstable (endemic case) when $\partial_{\Theta} f(\Theta)|_0 = 1$, which defines the critical parameters resulting in

$$\lambda_c = \frac{\langle k \rangle}{\langle k^2 \rangle - \langle k \rangle}, \quad (22)$$

where $\langle k \rangle$ is the average node degree and coincides with known results [29,30]. Equation (22) is also obtained analyzing the Jacobian of the linearized version of Eq. (18). It improves over the naive mean-field prediction $\lambda_c = \langle k \rangle / \langle k^2 \rangle$ [21]. The random regular graphs coincide with Table I since $\langle k^2 \rangle = \langle k \rangle^2$. For graphs with Poisson degree distribution (like Erdős-Rényi) $\langle k^2 \rangle = \langle k \rangle^2 + \langle k \rangle$ the epidemic threshold becomes $\lambda_c = \frac{1}{\langle k \rangle}$. For scale free graphs with power law distributed degrees, λ_c is finite whenever the second moment $\langle k^2 \rangle$ is finite. As is discussed in [20], these types of message passing approximations fail to predict a vanishing endemic threshold for scale free networks whose exponents are rather large.

A. General graph ensembles

Equations (17) and (18) are already a reduction of N differential equations to K average equations, where K is the

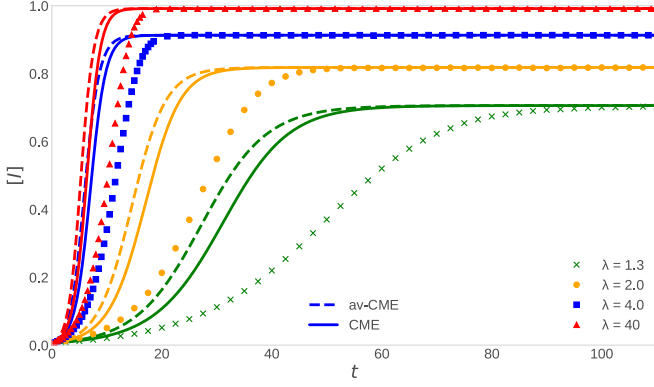


FIG. 5. Average probability of being infected as a function of time. The epidemic outbreak was in 10 nodes of each graph of 1000 nodes in an ensemble of 10 random regular graphs of connectivity 3. Each point of MC is an average over 10^4 simulations.

maximum degree in the graph. However, K itself could be large. We can further simplify by averaging now over the nodes degree and reducing to only two parameters $\tilde{p}_{\rightarrow} = \sum_{\gamma} g_{\text{link}}(\gamma) p_{\rightarrow}^{\gamma}$ and $\tilde{p} = \sum_{\gamma} P(\gamma) p^{\gamma}$:

$$\dot{\tilde{p}} = -\mu \tilde{p} + \beta \tilde{p}_{\rightarrow} \sum_{\gamma} (\gamma + 1) P(\gamma) (1 - p^{\gamma}), \quad (23)$$

$$\dot{\tilde{p}_{\rightarrow}} = -\mu \tilde{p}_{\rightarrow} + \beta \tilde{p}_{\rightarrow} \sum_{\gamma} \gamma g_{\text{link}}(\gamma) (1 - p_{\rightarrow}^{\gamma}). \quad (24)$$

These equations are still not closed, since the right hand sides still depend on the degree based parameters. The product by $(\gamma + 1)$ and γ inside the sums in the right hand sides does not allow for a direct connection with the definitions of \tilde{p} and \tilde{p}_{\rightarrow} . We will show, however, that in the case of Erdős-Rényi graphs such a connection can be obtained, though through some approximations and *Ansätze*.

A very simple case is that of regular graphs, where degree distribution is deltaic $P(\gamma) = g(\gamma) = \delta_{k-1, \gamma}$. Equations (17) and (18) reduce to two equations for the parameters $p^{k-1}(t) \equiv p(t)$ and $p_{\rightarrow}^{k-1}(t) \equiv p_{\rightarrow}(t)$:

$$\begin{aligned} \dot{\tilde{p}} &= -\mu \tilde{p} + \beta k \tilde{p}_{\rightarrow} (1 - p), \\ \dot{\tilde{p}_{\rightarrow}} &= -\mu \tilde{p}_{\rightarrow} + \beta (k - 1) \tilde{p}_{\rightarrow} (1 - p_{\rightarrow}), \end{aligned} \quad (25)$$

whose numerical integration can be compared with Monte Carlo simulations of epidemics in graphs with the same vertex degree k , and with the corresponding integration of the single instance CME equations (12) and (13). Figure 5 shows that the steady state is well predicted, while the transient is not, even in comparison with CME itself. This is a natural consequence of the loss of the spatial structure in the average case.

B. Closure on Erdős-Rényi graphs

For an Erdős-Rényi graph node degrees are Poisson distributed: $P(\gamma) = \frac{e^{-\kappa} \kappa^{\gamma}}{(\gamma+1)!}$ and $g_{\text{link}}(\gamma) = P(\gamma - 1)$, where κ is the average degree. We can connect the terms inside the sums in (23) and (24) with the derivatives of \tilde{p} and \tilde{p}_{\rightarrow} with respect to the parameter κ by noting

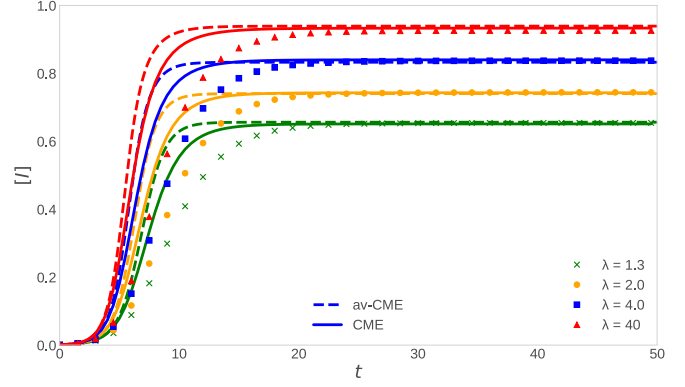


FIG. 6. Comparison between average-CME and CME for Erdős-Rényi graphs with mean connectivity (average degree) $\kappa = 3$, several values of μ , and $\beta = 0.4$. The figure shows the single site probability of infection as a function of time. As the ratio $\lambda = \beta/\mu$ decreases, the steady state has less infection probability. Each point of MC is an average over 10^4 simulations.

that

$$\frac{\partial \tilde{p}}{\partial \kappa} = -\tilde{p} + \frac{1}{\kappa} \sum_{\gamma} (\gamma + 1) P(\gamma) p^{\gamma}, \quad (26)$$

$$\frac{\partial \tilde{p}_{\rightarrow}}{\partial \kappa} = -\tilde{p}_{\rightarrow} + \frac{1}{\kappa} \sum_{\gamma} \gamma g_{\text{link}}(\gamma) p_{\rightarrow}^{\gamma}. \quad (27)$$

As shown in Appendix C, by substitution in (23) and (24) we get

$$\dot{\tilde{p}} = -\mu \tilde{p} + \beta \kappa \tilde{p}_{\rightarrow} \left[1 - \tilde{p} - \frac{\partial \tilde{p}}{\partial \kappa} \right], \quad (28)$$

$$\dot{\tilde{p}_{\rightarrow}} = [\beta \kappa - \mu] \tilde{p}_{\rightarrow} - \beta \kappa \tilde{p}_{\rightarrow} \left(\tilde{p}_{\rightarrow} + \frac{\partial \tilde{p}_{\rightarrow}}{\partial \kappa} \right). \quad (29)$$

In order to solve these equations we need some *Ansätze* for the dependence of the mean values \tilde{p} and \tilde{p}_{\rightarrow} on the mean degree in the graph. Inspired by the whole derivation of the cavity master equation for spin systems, we propose

$$\tilde{p}(t) = \frac{1}{2} \{ 1 + \tanh[\beta \kappa \chi(t) - \mu] \}, \quad (30)$$

$$\tilde{p}_{\rightarrow}(t) = \frac{1}{2} \{ 1 + \tanh[\beta \kappa \epsilon(t) - \mu] \}, \quad (31)$$

where $\chi(t)$ and $\epsilon(t)$ are some time-dependent fields that are obtained by inverting these very formulas in terms of \tilde{p} and \tilde{p}_{\rightarrow} .

From this *Ansatz* we can express the derivatives with respect to the degree in (28) and (29) in terms of \tilde{p} and \tilde{p}_{\rightarrow} , respectively (see Appendix C). We get then a closed system of differential equations for these probabilities, that can be solved numerically. The results of the integration are shown in Fig. 6.

VI. CONCLUSIONS

Analytical and numerical results have shown that the cavity master equation (CME) can be readily applied to effectively approximate the average dynamics of susceptible-infectious-susceptible models, where the average is intended over many

stochastic realizations of the epidemic process. The main contribution of this paper is methodological. CME corrects one term of the dynamic message passing equations previously derived in an intuitive way. Since CME is formally derived from a general framework, and since this correction produces a more accurate prediction when compared to numerical simulations, we retain CME to be the formal and correct way to derive message passing equations in epidemic models.

When compared to standard mean-field approaches, the takeaway message is nuanced. Numerical integration of CME equations on loopy graphs like random regular or Erdős-Rényi graphs are in good agreement with Monte Carlo predictions, especially for the steady state, and usually better than individual based mean field, rDMP, and a kind of pair-based mean field. Pair quenched mean field (PBMF-2) is still better than all these approximations, including CME. Furthermore, CME can be easily shown to drastically fail in graphs without loops or graphs where the ecochamber effect is fundamental, as in scale free networks.

Failure of CME on treelike topologies is all but expected, especially since the deduction of cavity equations in statistical mechanics is supposed to be exact on trees. Understanding what fails and when in the derivation of CME could open the way for better approximations in epidemics and beyond. The CME formalism has already been extended beyond the pair

approximation [31] (at some considerable computational cost) and the nonbacktracking feature disappears.

We also find appealing the applications of CME to multi-state models (Potts variables with q states) that would include the ubiquitous SIR and SIRS models. SIS epidemic models, for instance, are intrinsically nonbacktracking, since you cannot get infected again, and CME features could be less problematic in this setting.

ACKNOWLEDGMENTS

This research has received funding from the European Union's Horizon 2020 research and innovation programme MSCA-RISE-2016 under Grant Agreement No. 734439 INFERNET and also from the PNCB "Modelación matemática para la Epidemiología" from the Cuban Science Ministry. We are thankful to Dr. R. Mulet, Dr. C. Castellano, Dr. A. Vazquez, and Dr. C. Moore for useful discussions and comments to the manuscript.

APPENDIX A: CAVITY MASTER EQUATION FOR SIS MODEL

In this Appendix we will present more details on the formulation of the CME for the SIS model. Let us take as starting points Eqs. (10) and (11):

$$\frac{dP(\sigma_i)}{dt} = - \sum_{\sigma_{\partial i}} \left[r_i(\sigma_i, \sigma_{\partial i}) \left(\prod_{k \in \partial i} P(\sigma_k | \sigma_i) \right) P(\sigma_i) - r_i(-\sigma_i, \sigma_{\partial i}) \left(\prod_{k \in \partial i} P(\sigma_k | -\sigma_i) \right) P(-\sigma_i) \right], \quad (\text{A1})$$

$$\frac{dp(\sigma_i | \sigma_j)}{dt} = - \sum_{\sigma_{\partial i \setminus j}} \left[r_i[\sigma_i, \sigma_{\partial i}] \left(\prod_{k \in \partial i \setminus j} p(\sigma_k | \sigma_i) \right) p(\sigma_i | \sigma_j) - r_i[-\sigma_i, \sigma_{\partial i}] \left(\prod_{k \in \partial i \setminus j} p(\sigma_k | -\sigma_i) \right) p(-\sigma_i | \sigma_j) \right]. \quad (\text{A2})$$

Due to the complementarity of the probabilities $P_i(I)$ and $P_i(S)$ we can focus on just deriving the equation for one of the terms. Let us take $P_i(\sigma \equiv I)$ and rewrite Eq. (10) accordingly:

$$\frac{dP_i(I)}{dt} = - \sum_{\sigma_{\partial i}} \left[r_i(I, \sigma_{\partial i}) \left(\prod_{k \in \partial i} P_{ki}(\sigma | I) \right) P_i(I) - r_i(S, \sigma_{\partial i}) \left(\prod_{k \in \partial i} P_{ki}(\sigma_k | S) \right) P_i(S) \right]. \quad (\text{A3})$$

The rate $r_i(I, \sigma_{\partial i})$ is the transition rate from state $I \rightarrow S$ and in the SIS model and in most of the epidemic models it does not depend on the state of the contacts of the infected person. It just depends on the typical time of recovering (or dying) from the disease, so this rate is directly the recovering rate $r_i(I, \sigma_{\partial i}) = \mu$. On the other hand, $r_i(S, \sigma_{\partial i})$ is the transition rate from $S \rightarrow I$. In infectious diseases, the contagion can only occur if a susceptible individual is in contact with an infected one [$r_i(S, \sigma_k \equiv I) = \beta$, $r_i(S, \sigma_k \equiv S) = 0$], and the probability of getting infected is additive with the number of infected contacts. This means that we can rewrite $r_i(S, \sigma_{\partial i}) = \sum_{k \in \partial i} r_i(S, \sigma_k)$:

$$\begin{aligned} \frac{dP_i(I)}{dt} &= -\mu P_i(I) \sum_{\sigma_{\partial i}} \prod_{k \in \partial i} P_{ki}(\sigma | I) \\ &+ P_i(S) \sum_{\sigma_{\partial i}} \left[\sum_{k' \in \partial i} r_i(S, \sigma_{k'}) \right] \prod_{k \in \partial i} P_{ki}(\sigma_k | S). \end{aligned} \quad (\text{A4})$$

Let us apply the equivalence $\sum_{\sigma_{\partial i}} \prod_{k \in \partial i} \rightarrow \prod_{k \in \partial i} \sum_{\sigma_k}$ to invert the sum and product in the first term of the right hand side (RHS):

$$\begin{aligned} \frac{dP_i(I)}{dt} &= -\mu P_i(I) \prod_{k \in \partial i} \left[\sum_{\sigma_k} P_{ki}(\sigma | I) \right] \\ &+ P_i(S) \sum_{\sigma_{\partial i}} \left[\sum_{k' \in \partial i} r_i(S, \sigma_{k'}) \right] \prod_{k \in \partial i} P_{ki}(\sigma_k | S). \end{aligned} \quad (\text{A5})$$

The term $\sum_{\sigma_k} P_{ki}(\sigma | I)$ is exactly the sum of $P_{ki}(I|I) + P_{ki}(S|I) = 1$ and therefore also the product is equal to 1:

$$\frac{dP_i(I)}{dt} = -\mu P_i(I) + P_i(S) \sum_{\sigma_{\partial i}} \left[\sum_{k' \in \partial i} r_i(S, \sigma_{k'}) \right] \prod_{k \in \partial i} P_{ki}(\sigma_k | S). \quad (\text{A6})$$

Now we rewrite the second term of the RHS as follows:

$$\frac{dP_i(I)}{dt} = -\mu P_i(I) + P_i(S) \sum_{\sigma_{ai}} \sum_{k' \in \partial i} r_i(S, \sigma_{k'}) P_{k'i}(\sigma | S) \times \prod_{k \in \partial i \setminus k'} P_{ki}(\sigma | S), \quad (\text{A7})$$

$$\frac{dP_i(I)}{dt} = -\mu P_i(I) + P_i(S) \sum_{\sigma_{k'}} \sum_{k' \in \partial i} r_i(S, \sigma_{k'}) P_{k'i}(\sigma | S) \times \sum_{\sigma_{ai \setminus k'}} \prod_{k \in \partial i \setminus k'} P_{ki}(\sigma | S). \quad (\text{A8})$$

Exchanging again the sum and the product, but now on the last term, we get $\sum_{\sigma_{ai \setminus k'}} [\prod_{k \in \partial i \setminus k'} P_{ki}(\sigma | S)] = 1$ and, using that $r_i(S, S) = 0$ and $r_i(S, I) = \beta$, we obtain Eq. (12):

$$\frac{dp_i}{dt} = -\mu p_i + \beta(1 - p_i) \sum_k p_{ki}. \quad (\text{A9})$$

Following the same steps it is easy to derive Eq. (13) for conditional probabilities.

APPENDIX B: AVERAGE CASE EQUATIONS FOR ERDŐS-RÉNYI GRAPHS

In this Appendix we will show how to perform the closure of average-case equations for Erdős-Rényi graphs (Sec. VB). Let us start by explicitly writing the derivatives with respect to κ :

$$\frac{\partial \tilde{p}}{\partial \kappa} = \frac{\partial}{\partial \kappa} \left(\sum_{\gamma} P(\gamma) p^{\gamma} \right) = \frac{\partial}{\partial \kappa} \left(\sum_{\gamma} \frac{e^{-\kappa} \kappa^{\gamma+1}}{(\gamma+1)!} p^{\gamma} \right), \quad (\text{B1})$$

$$\frac{\partial \tilde{p}_{\rightarrow}}{\partial \kappa} = \frac{\partial}{\partial \kappa} \left(\sum_{\gamma} g_{\text{link}}(\gamma) p_{\rightarrow}^{\gamma} \right) = \frac{\partial}{\partial \kappa} \left(\sum_{\gamma} \frac{e^{-\kappa} \kappa^{\gamma}}{\gamma!} p_{\rightarrow}^{\gamma} \right). \quad (\text{B2})$$

Computation of (B1) and (B2) gives

$$\begin{aligned} \frac{\partial \tilde{p}}{\partial \kappa} &= - \sum_{\gamma} \frac{e^{-\kappa} \kappa^{\gamma+1}}{(\gamma+1)!} p^{\gamma} + \sum_{\gamma} (\gamma+1) \frac{e^{-\kappa} \kappa^{\gamma}}{(\gamma+1)!} p^{\gamma} \\ &= -\tilde{p} + \frac{1}{\kappa} \sum_{\gamma} (\gamma+1) P(\gamma) p^{\gamma}, \end{aligned} \quad (\text{B3})$$

$$\begin{aligned} \frac{\partial \tilde{p}_{\rightarrow}}{\partial \kappa} &= - \sum_{\gamma} \frac{e^{-\kappa} \kappa^{\gamma}}{(\gamma)!} p_{\rightarrow}^{\gamma} + \sum_{\gamma} \gamma \frac{e^{-\kappa} \kappa^{\gamma-1}}{\gamma!} p_{\rightarrow}^{\gamma} \\ &= -\tilde{p}_{\rightarrow} + \frac{1}{\kappa} \sum_{\gamma} \gamma g_{\text{link}}(\gamma) p_{\rightarrow}^{\gamma}. \end{aligned} \quad (\text{B4})$$

The sums in the right hand sides of (B3) and (B4) are also involved in Eqs. (23) and (24). Then, remembering that $\kappa = \sum_{\gamma} (\gamma+1) P(\gamma)$, we can rewrite Eq. (23) as

follows:

$$\begin{aligned} \dot{\tilde{p}} &= -\mu \tilde{p} + \beta \tilde{p}_{\rightarrow} \sum_{\gamma} (\gamma+1) P(\gamma) (1 - p^{\gamma}), \\ \dot{\tilde{p}} &= -\mu \tilde{p} + \beta \tilde{p}_{\rightarrow} \sum_{\gamma} (\gamma+1) P(\gamma) \\ &\quad - \beta \tilde{p}_{\rightarrow} \sum_{\gamma} (\gamma+1) P(\gamma) p^{\gamma}, \\ \dot{\tilde{p}} &= -\mu \tilde{p} + \beta \kappa \tilde{p}_{\rightarrow} - \beta \kappa \tilde{p}_{\rightarrow} \left(\tilde{p} + \frac{\partial \tilde{p}}{\partial \kappa} \right), \end{aligned} \quad (\text{B5})$$

which leads directly to Eq. (28). Equation (29) can be derived by an analogous procedure, using an equivalent expression for the mean connectivity: $\kappa = \sum_{\gamma} \gamma g_{\text{link}}(\gamma)$.

Now we just need to obtain closed expressions for the derivatives in (28) and (29). In order to do so, let us compute the κ derivative on both sides of *Ansätze* (30) and (31). We get

$$\frac{\partial \tilde{p}}{\partial \kappa} = \frac{1}{2} \{1 - \tanh^2 [\beta \kappa \chi(t) - \mu]\} \beta \chi(t), \quad (\text{B6})$$

$$\frac{\partial \tilde{p}_{\rightarrow}}{\partial \kappa} = \frac{1}{2} \{1 - \tanh^2 [\beta \kappa \epsilon(t) - \mu]\} \beta \epsilon(t). \quad (\text{B7})$$

We can reuse Eqs. (30) and (31) for eliminating $\chi(t)$ and $\epsilon(t)$ from (B6) and (B7), thus obtaining the following closed expressions for the derivatives:

$$\frac{\partial \tilde{p}}{\partial \kappa} = \frac{1}{2\kappa} [1 - (2\tilde{p} - 1)^2] [\tanh^{-1}(2\tilde{p} - 1) + \mu], \quad (\text{B8})$$

$$\frac{\partial \tilde{p}_{\rightarrow}}{\partial \kappa} = \frac{1}{2\kappa} [1 - (2\tilde{p}_{\rightarrow} - 1)^2] [\tanh^{-1}(2\tilde{p}_{\rightarrow} - 1) + \mu]. \quad (\text{B9})$$

This allows us to numerically solve Eqs. (28) and (29).

APPENDIX C: ANALYTICAL DIFFERENCE BETWEEN PBMF-2 AND CME

To understand the difference between PBMF-2 and CME we need to have both approximations with the same notation, meaning that we have to put both in the notation of the joint probabilities or in the notation of the conditional probabilities. Here we are going to translate the equations of PBMF-2 into the conditional probabilities notation:

$$\begin{aligned} \frac{d\phi_{ij}(t)}{dt} &= \frac{d\rho_{ij}q_j}{dt} \\ &= \frac{d\rho_{ij}}{dt} q_j + \frac{dq_j}{dt} \rho_{ij}. \end{aligned} \quad (\text{C1})$$

Therefore,

$$\frac{d\rho_{ij}}{dt} = \frac{d\phi_{ij}(t)}{dt} \frac{1}{q_j} - \frac{dq_j}{dt} \frac{\rho_{ij}}{q_j}. \quad (\text{C2})$$

Let us rewrite the set of equations (6) of PBMF-2 in terms of the individual probability of being susceptible q_i instead of the individual probability of being infected:

$$\frac{dq_i(t)}{dt} = \mu [1 - q_i(t)] - \beta \sum_{j \in \partial i} \phi_{ij}(t),$$

$$\begin{aligned} \frac{d\phi_{ij}(t)}{dt} &= -(2\mu + \beta)\phi_{ij}(t) + \mu[1 - \varrho_i(t)] - \beta\phi_{ij}(t)/(\varrho_j) \\ &\times \sum_{k \in \partial j \setminus i} \phi_{kj}(t) + \beta[\varrho_i(t) - \phi_{ij}(t)] \sum_{k \in \partial i \setminus j} \phi_{ki}/(\varrho_i)(t). \end{aligned} \quad (\text{C3})$$

In terms of the conditional probability the join probability then takes the form

$$\begin{aligned} \frac{d\phi_{ij}(t)}{dt} &= -(2\mu + \beta)\rho_{ij}(t)\varrho_j(t) + \mu[1 - \varrho_i(t)] \\ &- \beta\rho_{ij}(t)\varrho_j(t)/(\varrho_j)(t) \sum_{k \in \partial j \setminus i} \rho_{kj}(t)\varrho_j(t) \\ &+ \beta[\varrho_j(t) - \rho_{ij}(t)\varrho_j(t)] \sum_{k \in \partial i \setminus j} \rho_{ki}(t)\varrho_i(t)/(\varrho_i)(t). \end{aligned} \quad (\text{C4})$$

Then,

$$\begin{aligned} \frac{d\phi_{ij}(t)}{dt} \frac{1}{\varrho_j(t)} &= -(2\mu + \beta)\rho_{ij}(t) + \frac{\mu[1 - \varrho_i(t)]}{\varrho_j(t)} \\ &- \beta\rho_{ij}(t) \sum_{k \in \partial j \setminus i} \rho_{kj}(t) \\ &+ \beta[1 - \rho_{ij}(t)] \sum_{k \in \partial i \setminus j} \rho_{ki}(t), \end{aligned} \quad (\text{C5})$$

and the time derivative of the individual probability of being susceptible times the conditional probability

and divided by the individual probability of being susceptible is

$$\begin{aligned} -\frac{d\varrho_j(t)}{dt} \frac{\rho_{ij}(t)}{\varrho_j(t)} &= -\mu[1 - \varrho_j(t)] \frac{\rho_{ij}(t)}{\varrho_j(t)} + \beta\rho_{ij}(t) \\ &\times \sum_{k \in \partial i \setminus j} \rho_{kj}(t) + \beta\rho_{ij}(t)\rho_{ij}(t). \end{aligned} \quad (\text{C6})$$

Adding (C5) and (C6) we get

$$\begin{aligned} \frac{d\rho_{ij}}{dt} &= -(2\mu + \beta)\rho_{ij}(t) + \frac{\mu[1 - \varrho_i(t)]}{\varrho_j(t)} \\ &- \mu[1 - \varrho_j(t)] \frac{\rho_{ij}(t)}{\varrho_j(t)} + \beta[1 - \rho_{ij}(t)] \sum_{k \in \partial i \setminus j} \rho_{ki} \\ &+ \beta\rho_{ij}(t)\rho_{ij}(t). \end{aligned} \quad (\text{C7})$$

Finally, let us rewrite it to see which terms are missing in CME:

$$\begin{aligned} \frac{d\rho_{ij}}{dt} &= -\mu\rho_{ij}(t) + \beta[1 - \rho_{ij}(t)] \\ &\times \sum_{k \in \partial i \setminus j} \rho_{ki} + \frac{\mu\rho_i(t)}{\varrho_j(t)} \\ &- \mu \frac{\rho_{ij}(t)}{\varrho_j(t)} + \beta\rho_{ij}(t)\rho_{ij}(t) - \beta\rho_{ij}(t). \end{aligned} \quad (\text{C8})$$

-
- [1] W. O. Kermack and A. G. McKendrick, A contribution to the mathematical theory of epidemics, *Proc. R. Soc. London A* **115**, 700 (1927).
- [2] C. C. Kerr, R. M. Stuart, D. Mistry, R. G. Abeysuriya, G. Hart, K. Rosenfeld, P. Selvaraj, R. C. Nunez, B. Hagedorn, L. George *et al.*, Covasim: An agent-based model of covid-19 dynamics and interventions, *PLOS Comput. Biology* **17**, e1009149 (2021).
- [3] E. Cuevas, An agent-based model to evaluate the covid-19 transmission risks in facilities, *Comput. Biol. Med.* **121**, 103827 (2020).
- [4] R. Hinch, W. J. M. Probert, A. Nurta, M. Kendall, C. Wymatt, M. Hall, K. Lythgoe, A. B. Cruz, L. Zhao, A. Stewart *et al.*, OpenABM-covid19-an agent-based model for non-pharmaceutical interventions against covid-19 including contact tracing, *PLoS Comput. Biology* **17**, e1009146 (2021).
- [5] TBfP. L. Simon, M. Taylor, and I. Z. Kiss, Exact epidemic models on graphs using graph-automorphism driven lumping, *J. Math. Biol.* **62**, 479 (2011).
- [6] F. D. Sahneh, C. Scoglio, and P. V. Mieghem, Generalized epidemic mean-field model for spreading processes over multilayer complex networks, *IEEE/ACM Trans. Netw.* **21**, 1609 (2013).
- [7] A. Y. Lokhov, M. Mézard, H. Ohta, and L. Zdeborová, Inferring the origin of an epidemic with a dynamic message-passing algorithm, *Phys. Rev. E* **90**, 012801 (2014).
- [8] M. Shrestha, S. V. Scarpino, and C. Moore, Message-passing approach for recurrent-state epidemic models on networks, *Phys. Rev. E* **92**, 022821 (2015).
- [9] F. Altarelli, A. Braunstein, L. Dall'Asta, A. Lage-Castellanos, and R. Zecchina, Bayesian Inference of Epidemics on Networks via Belief Propagation, *Phys. Rev. Lett.* **112**, 118701 (2014).
- [10] A. Braunstein and A. Ingrosso, Inference of causality in epidemics on temporal contact networks, *Sci. Rep.* **6**, 27538 (2016).
- [11] A. Baker, I. Biazzo, A. Braunstein, G. Catania, L. Dall'Asta, A. Ingrosso, F. Krzakala, F. Mazza, M. Mézard, A. P. Muntoni *et al.*, Epidemic mitigation by statistical inference from contact tracing data, *Proc. Natl. Acad. Sci. USA* **118**, e2106548118 (2021).
- [12] G. Bianconi, H. Sun, G. Rapisardi, and A. Arenas, Message-passing approach to epidemic tracing and mitigation with apps, *Phys. Rev. Research* **3**, L012014 (2021).
- [13] W. Krauth and M. Mézard, The cavity method and the travelling-salesman problem, *Europhys. Lett.* **8**, 213 (1989).
- [14] E. Aurell, G. D. Ferraro, E. Domínguez, and R. Mulet, Cavity master equation for the continuous time dynamics of discrete-spin models, *Phys. Rev. E* **95**, 052119 (2017).
- [15] E. Cator and P. V. Mieghem, Second-order mean-field susceptible-infected-susceptible epidemic threshold, *Phys. Rev. E* **85**, 056111 (2012).
- [16] A. S. Mata and S. C. Ferreira, Pair quenched mean-field theory for the susceptible-infected-susceptible model on complex networks, *Europhys. Lett.* **103**, 48003 (2013).

- [17] D. H. Silva, S. C. Ferreira, W. Cota, R. Pastor-Satorras, and C. Castellano, Spectral properties and the accuracy of mean-field approaches for epidemics on correlated power-law networks, *Phys. Rev. Research* **1**, 033024 (2019).
- [18] D. H. Silva, F. A. Rodrigues, and S. C. Ferreira, High prevalence regimes in the pair-quenched mean-field theory for the susceptible-infected-susceptible model on networks, *Phys. Rev. E* **102**, 012313 (2020).
- [19] K. J. Sharkey, Deterministic epidemiological models at the individual level, *J. Math. Biol.* **57**, 311 (2008).
- [20] C. Castellano and R. Pastor-Satorras, Relevance of backtracking paths in recurrent-state epidemic spreading on networks, *Phys. Rev. E* **98**, 052313 (2018).
- [21] R. Pastor-Satorras, C. Castellano, P. V. Mieghem, and A. Vespignani, Epidemic processes in complex networks, *Rev. Mod. Phys.* **87**, 925 (2015).
- [22] S. C. Ferreira, C. Castellano, and R. Pastor-Satorras, Epidemic thresholds of the susceptible-infected-susceptible model on networks: A comparison of numerical and theoretical results, *Phys. Rev. E* **86**, 041125 (2012).
- [23] J. P. Gleeson, Binary-State Dynamics on Complex Networks: Pair Approximation and Beyond, *Phys. Rev. X* **3**, 021004 (2013).
- [24] A. V. Goltsev, S. N. Dorogovtsev, J. G. Oliveira, and J. F. F. Mendes, Localization and Spreading of Diseases in Complex Networks, *Phys. Rev. Lett.* **109**, 128702 (2012).
- [25] P. V. Mieghem, Epidemic phase transition of the sis type in networks, *Europhys. Lett.* **97**, 48004 (2012).
- [26] R. Pastor-Satorras and A. Vespignani, Epidemic Spreading in Scale-Free Networks, *Phys. Rev. Lett.* **86**, 3200 (2001).
- [27] R. Pastor-Satorras and A. Vespignani, Optimal immunisation of complex networks, *Phys. Rev. E* **65**, 036104 (2002).
- [28] R. Pastor-Satorras and A. Vespignani, Epidemic dynamics and endemic states in complex networks, *Phys. Rev. E* **63**, 066117 (2001).
- [29] A. S. Mata, R. S. Ferreira, and S. C. Ferreira, Heterogeneous pair-approximation for the contact process on complex networks, *New J. Phys.* **16**, 053006 (2014).
- [30] C.-R. Cai, Z.-X. Wu, M. Z. Q. Chen, P. Holme, and J.-Y. Guan, Solving the Dynamic Correlation Problem of the Susceptible-Infected-Susceptible Model on Networks, *Phys. Rev. Lett.* **116**, 258301 (2016).
- [31] D. Machado and R. Mulet, From random point processes to hierarchical cavity master equations for stochastic dynamics of disordered systems in random graphs: Ising models and epidemics, *Phys. Rev. E* **104**, 054303 (2021).